EPSC Abstracts
Vol. 13, EPSC-DPS2019-617-1, 2019
EPSC-DPS Joint Meeting 2019

EPSC
EPSC-DPS Joint Meeting 2019
15–20 September 2019 | Geneva, Switzerland

The HP³ Radiometer on InSight

N.T. Mueller (1), M. Grott (1), S. Piqueux (2), T. Spohn (1,3), S.E. Smrekar (2), J. Knollenberg (1), T.L. Hudson (2), A. Spiga (4), F. Forget (4), E. Millour (4), M. Lemmon (5), J. Maki (2), M. Golombek (2), W.B. Banerdt(2)
(1) German Aerospace Center (DLR), Institute of Planetary Research, Berlin, Germany, (2) Jet Propulsion Laboratory, California Institute of Technology, Pasadena, CA, USA, (3) International Space Science Institute, Bern, Switzerland, (4) Laboratoire de Météorologie Dynamique (LMD/IPSL) Sorbonne Université, Paris, France, (5)Texas A&M University, Department of Atmospheric Science, College Station, TX, USA. Nils.Mueller@dlr.de

Abstract

The Heat Flow and Physical Properties Package (HP³) [1] includes an infrared Radiometer attached to the deck of the InSight lander [2]. The main objective of this part of the instrument is to constrain the surface thermal boundary condition for the heat flow derivation by the instrumented tether deployed into the subsurface. The heat flow in the subsurface can be affected by seasonal and diurnal temperature variations, by radiation from the lander, its shadow, and the change in surface albedo caused by dust removal during landing and later deposition. The radiometer will observe the seasonal variation over the course of the mission. Fitting of diurnal temperature curves provides an estimate of albedo and other thermophysical properties of the near surface, and possibly constrains atmospheric variables such as the ratio of visible to infrared dust opacity.

1. HP³ RAD

The design is based on the MAscot RAdiometer (MARA) [3] and uses 6 thermopile sensors in a temperature stabilized sensor head. The thermopile sensors consist of a set of thermocouples with a hot junction in radiative heat exchange with the outside through a spectral bandpass filter. The instrument temperature is stabilized by controlled heating to a temperature setpoint above the equilibrium temperature. The instrument observes two spots on the surface with 3 sensors each. The three sensors have different spectral bandpasses: 8-14, 8-10 and 16-19 µm. The two spots observed by the radiometer are in approximately 1.5 and 3 m distance N-N-W from the lander center (Fig. 1). At the beginning and the end of the nominal mission, the shadows of the solar panels pass over the closer spot in the morning and afternoon (Fig. 2).

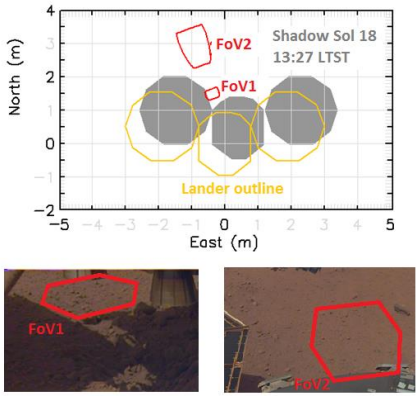

Figure 1: *Top: Plan view of the location of the radiometer footprints (red). Bottom: Arm camera images of the RAD spots.*

2. Data and performance

From opening of the dust cover on sol 14 to sol 150 RAD acquired hourly data on most sols. On sol 39 data were acquired continuously with higher sampling rate over the afternoon to observe the passage of the shadow through the near spot in more detail. On sols 79-80 and sols 119-120, observations of the full diurnal cycle were carried out to compare with wind and atmosphere temperature data from TWINS [4] and obtain diagnostics on how near-surface (in)stability drives the Planetary Boundary Layer dynamics [5]. On sols 96, 97 and 99 high sampling rate data were acquired during three Phobos eclipses and significant responses were detected except for the last one, which was late in the afternoon. Calibration data were acquired in regular intervals of ~30 sols and show so far no sensor degradation after landing. The calibration uncertainties are less than 4 K for the 8-14 µm filters in the worst case (+25C instrument temperature setpoint in the late afternoon) and noise is less than the equivalent temperature difference of 0.5K.

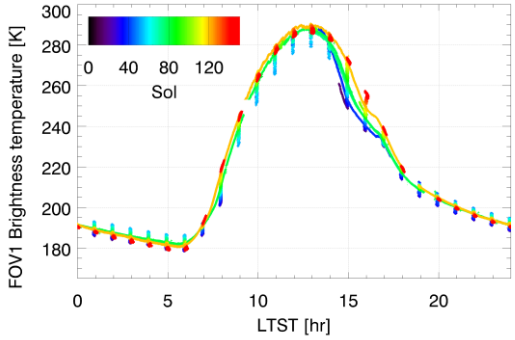

Figure 2: *8-14µm data measured at the spot near the lander (FoV1).*

3. Initial Results

The diurnal temperature response provides an estimate of the thermal inertia, which is a diagnostic of soil parameters such as grain size and cementation. We use output from the LMD1D model (a 1D version of the model described in [6]) as boundary conditions to solve the heat conduction in the near surface and to calculate model curves of surface temperature. The model accounts for the Mars orbit and provides downwelling solar and infrared fluxes. Atmospheric dust opacity is derived from camera images of the sky [7]. We vary the input thermal inertia to find the diurnal and eclipse responses that match the data well (Fig. 3). The diurnal curve on sol 97 indicates a thermal inertia of ~200$Jm^{-2}K^{-1}s^{-1/2}$ however the eclipse response indicates that there might be some different material (~120$Jm^{-2}K^{-1}s^{-1/2}$) at the surface. The temperature after the eclipse appears to return to normal values faster than predicted, which might indicate that only a fraction of the footprint is covered with different material, however in this case with an even lower thermal inertia. The bulk thermal inertia is consistent with orbiter observations and indicates material particle size in the range of sand, and little cementation [8]. On other sols the diurnal curve is fitted less well with the same surface parameters. Since the surface parameters can be assumed constant, it is likely that we have not yet accurately accounted for all atmospheric variables. One of these parameters may be the ratio of visible to infrared dust opacity, which we assumed to be constant at a value of 2. The MER rovers with the capability to measure opacity in both bands showed that this ratio varies [7]. Initial modeling shows that varying this ratio improves the model fits so that we might be able to derive this ratio as a time series.

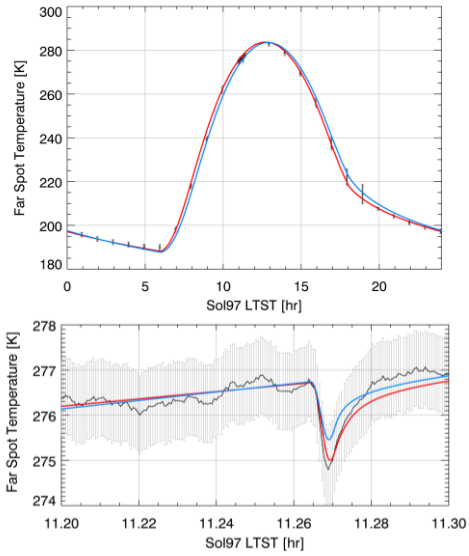

Figure 3: *Far spot observations on sol 97 with 1-sigma errors bars. Blue: model curve based on the LMD1D model radiative fluxe, modified to include the eclipse, and a surface with albedo 0.2 and thermal inertia of 200 $Jm^{-2}K^{-1}s^{-1/2}$. Red: model curve based on the same boundary conditions and a 6mm thick layer of lower thermal inertia material (120$Jm^{-2}K^{-1}s^{-1/2}$) at the surface. Models are offset by +1.2 and -0.7 K to match temperatures at the beginning of the eclipse for better comparison of amplitudes*

References

[1] Spohn, T. et al., Space Sci. Rev., 214:96 (2018).

[2] Banerdt, W.B., et al., Space Sci. Rev., 211, 1–3 (2017).

[3] Grott, M. et al. Space Sci. Rev. 208:413 (2017).

[4] Banfield, D. et al., Space Sci. Rev., 215:4 (2018).

[5] Spiga, A. et al. Space Sci. Rev., Space Science Reviews, 214:109 (2018).

[6] Forget, F. et al., JGR 104:E10, 24155-24175 (1999).

[7] Lemmon et al., Icarus 251,96 (2015).

[8] Piqueux, S. & Christensen, P.R. JGR, 116:E07004 (2011).